

The role of fire on soil mounds and surface roughness in the Mojave Desert

Christopher E. Soulard,^{1*} Todd C. Esque,² David R. Bedford³ and Sandra Bond⁴

¹ Western Geographic Science Center, United States Department of the Interior, United States Geological Survey, Menlo Park, CA, USA

² Western Ecological Research Center, Las Vegas Field Station, United States Department of the Interior, United States Geological Survey, Henderson, NV, USA

³ Geology, Energy, Minerals, and Geophysics Science Center, United States Department of the Interior, United States Geological Survey, Menlo Park, CA, USA

⁴ Western Remote Sensing and Visualization Center, United States Department of the Interior, United States Geological Survey, Sacramento, CA, USA

Received 18 November 2011; Revised 20 April 2012; Accepted 25 April 2012

*Correspondence to: Christopher E. Soulard, Western Geographic Science Center, United States Department of the Interior, United States Geological Survey, 345 Middlefield Road, MS-531, Menlo Park, CA 94025, USA. E-mail: csoulard@usgs.gov

ESPL

Earth Surface Processes and Landforms

ABSTRACT: A fundamental question in arid land management centers on understanding the long-term effects of fire on desert ecosystems. To assess the effects of fire on surface topography, soil roughness, and vegetation, we used terrestrial (ground-based) LiDAR to quantify the differences between burned and unburned surfaces by creating a series of high-resolution vegetation structure and bare-earth surface models for six sample plots in the Grand Canyon-Parashant National Monument, Arizona. We find that 11 years following prescribed burns, mound volumes, plant heights, and soil-surface roughness were significantly lower on burned relative to unburned plots. Results also suggest a linkage between vegetation and soil mounds, either through accretion or erosion mechanisms such as wind and/or water erosion. The biogeomorphic implications of fire-induced changes are significant. Reduced plant cover and altered soil surfaces from fire likely influence seed residence times, inhibit seed germination and plant establishment, and affect other ecohydrological processes. Published in 2012. This article is a US Government work and is in the public domain in the USA.

KEYWORDS: TLS; LiDAR; fire; Mojave Desert; surface roughness; topography

Introduction

In desert shrublands, soil properties beneath perennial shrubs differ in structure and composition from interspaces and are important ecosystem features formed by dust deposition, rain splash, the activities of animals, or residual erosion (Schlesinger *et al.*, 1990; Bochet *et al.*, 2000; Titus *et al.*, 2002). Vegetation is commonly present on plant mounds, also known as coppice mounds, hillocks, or microspheres (Abrahams *et al.*, 1995; Bochet *et al.*, 2000). Mounds are important because they are nutrient rich and can contain more organic matter and water content, serving as sources of plant fertility (Abrahams *et al.*, 1995; Schlesinger and Pilmanis, 1998; Reynolds *et al.*, 1999). One process that has immediate and potentially permanent effects on soil geomorphology and the quantity, quality, and fertility of plants in arid landscapes is fire (Okin *et al.*, 2009). Fire can change the chemical composition and hydrologic properties of the soils in plant mounds (Ravi *et al.*, 2009; Esque *et al.*, 2010a). Roughness of the soil surface can also vary in response to fire, wind, or water erosion, and changes are enhanced by the loss of vegetation (Boxell and Drohan, 2009) and mineral or biotic crusts that protect surfaces from the elements (Pierson *et al.*, 2002; Belnap and Lange, 2003; Ravi *et al.*, 2009). Potential losses of soil-surface roughness

may reduce the residence time for seeds in a burned area, as seeds reside on rougher surfaces longer (van den Berg and Kellner, 2005; DeFalco *et al.*, 2010). Monitoring the impact of fire on desert vegetation and geomorphology long after fires occur may provide insights into the decline of land productivity and further desertification.

Changes in the volume of mound features and roughness of soil surfaces have not commonly been quantified previously due to technological limitations. Until recently, large-scale soil surface analyses were primarily studied using aerial photograph interpretation and traditional surveying techniques (Nizeyimana and Petersen, 1998), with radar (Rahman *et al.*, 2008) and satellite data (Jackson *et al.*, 1982) reserved for watershed-to-regional scale studies. Such analyses were significantly improved with the advent of airborne light detection and ranging (LiDAR) and high-precision, high-accuracy global positioning system (GPS), which have provided scientists with improved tools to remotely study shrub and soil characteristics at a fine scale and high precision (Ritchie, 1995; Frankel and Dolan, 2007; Sankey *et al.*, 2010; Sankey and Bond, 2011). These technologies have continued to evolve, becoming more precise while introducing alternative methods to address scientific questions. They have also given rise to new scientific tools in recent years, specifically terrestrial LiDAR (t-LiDAR),

also known as terrestrial laser scanning (TLS) or ground-based LiDAR. In contrast to airborne systems, t-LiDAR instruments are portable, mounted on tripods, and provide higher-precision measurements (i.e. millimeter point spacing). They utilize the time delay of the reflection of pulses of light from target surfaces to measure distance. T-LiDAR point data have enabled scientists to build high-resolution three-to-four-dimensional (the fourth dimension is a measurement of point intensity) models of objects of interest. Recently, t-LiDAR technology has been used in a small number of soil roughness studies (Perez-Gutierrez *et al.*, 2007; Haubrock *et al.*, 2009; Li *et al.*, 2010; Eitel *et al.*, 2011; Sankey *et al.*, 2011). High-resolution, soil roughness measurements with higher precision can be used to improve sediment and hydrological process modeling outputs by reducing uncertainty and contribute to the overall understanding of biogeomorphic processes following disturbances (Sankey *et al.*, 2011).

Although it is well established that many of the shrub communities in the northern Sonoran and Chihuahuan Deserts of the arid southwest were formerly grasslands (Hastings and Turner, 1965; Cox *et al.*, 1983), large parts of the Mojave Desert have been characterized by a shrubby landscape composition for at least 6000 years (Spaulding, 1990). The shrubby vegetation (*Larrea tridentata* and *Ambrosia dumosa* shrubs in this case) that covers the Mojave Desert tends to be located in association with mounds that are generally small in size (at less than a meter in diameter). The spatial resolution of t-LiDAR (in millimeters) and the ability to resolve mound dimensions beneath shrub cover present an opportunity to measure differences in the volume and surface roughness of soil mounds between burned and unburned sample plots without physically removing or manipulating the overlying vegetation. In this study, we use t-LiDAR to quantify differences in soil topography in burned and unburned areas following 11 years of recovery to identify if fire impacts soil-surface roughness. Our objectives were to: (1) examine whether topographical differences in mound volume and surface roughness exist between burned and unburned surfaces, and (2) test the hypotheses that soil mound volume and surface roughness decrease following the removal of vegetation by fire. Our hypotheses are grounded in other research where burning shrublands led to flatter disturbed surfaces (Hilty *et al.*, 2003),

or where homogenization occurred on burned landscapes where wind transported and deposited sediment from formerly vegetated mounds into interspaces (Ravi *et al.*, 2009). Past research has also made alternative conclusions, either finding that surface roughness varied between study sites depending on localized differences in erosional and depositional patterns (Sankey *et al.*, 2010) or that burning had a scale-dependent influence on surface roughness, contributing to more roughness on mounds while leading to smoother surfaces at the plot scale (Sankey *et al.*, 2011).

Study area

The study area is located in Grand Canyon-Parashant National Monument, Mohave County, Arizona (36°25'N, 113°55'W), 50 km south of Littlefield, Arizona (Figure 1). Site elevations range from 800 to 1000 m. From 1957 to 1992, 60% (Esque *et al.*, 2010a) of the annual 208 ± 15 mm precipitation (NOAA, 2003) fell in winter. Mojave Desert shrub assemblages of *Larrea tridentata* and *Ambrosia dumosa* dominate the area (Brown, 1982). Perennial plant cover ranges from 6% to 20% across the area (Esque, 2004). Soils on the mesa are in the Winkel series of loamy-skeletal, mixed, superactive, thermic, shallow Calcic Petrocalcids. The typical surface soil pH is 8.8 for this series. The study plots occur atop a north-south trending basalt mesa (i.e. inverted paleovalley) with soil depth ranging from 30 to 50 cm.

Prescribed fires were conducted over 10 days in September 1998. A grass hay fuel load was applied at the concentration of 3175 kg/ha to completely cover aboveground spring annual plant production in the region (Esque *et al.*, 2010b). According to field photographs, the maximum flame length was variable, ranging from 2 to 3 m around burning shrubs to 0.5 to 1.0 m for interspaces. Mean peak temperatures varied by cover type: *Ambrosia* was 579 ± 132 °C, *Larrea* was 445 ± 144 °C, and interspaces were 399 ± 88 °C (Esque *et al.*, 2010b).

The prescribed fires caused damage to all foliage and exfoliation of all perennial plants within the plots. Acknowledging that some smaller portion of perennial cover loss was attributed to drought (Esque, 2004), the net loss of perennial plant cover

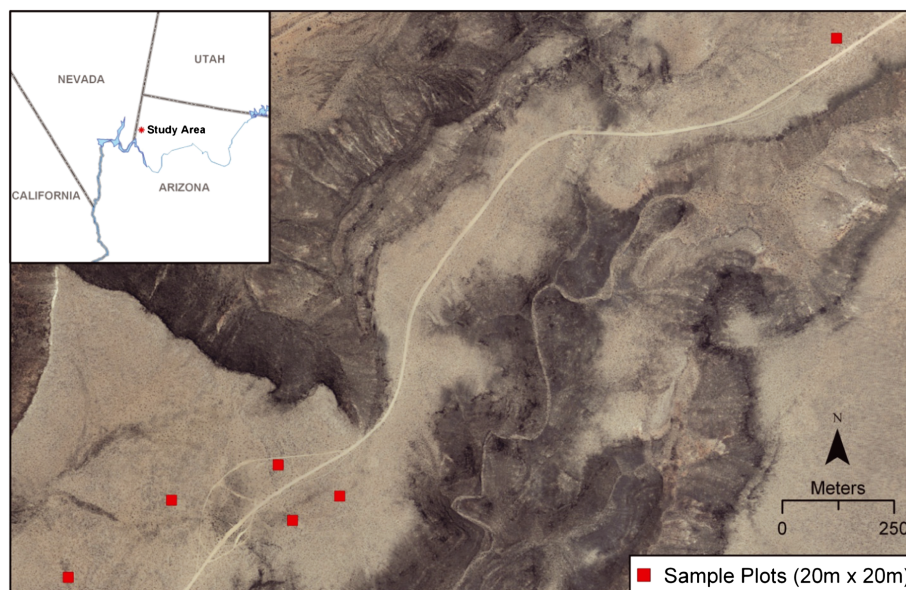


Figure 1. As part of a larger study, plots were established within six locations dispersed along 7 km of a graded road. Three plots were randomly assigned burned and three assigned unburned treatments. This study was conducted at Grand Canyon-Parashant National Monument, Arizona in Mojave Desert. Base imagery is from the 2007 National Agricultural Imagery Program (USDA, 2007). This figure is available in colour online at wileyonlinelibrary.com/journal/espl

Table I. Mean percent cover of *Ambrosia dumosa* and *Larrea tridentata* by burning treatment and year

Plot	<i>Ambrosia</i>	<i>Larrea</i>	<i>Ambrosia</i>	<i>Larrea</i>	<i>Ambrosia</i>	<i>Larrea</i>
	1998 (prior to burn)	1998 (prior to burn)	2000 (after burn)	2000 (after burn)	2001 (after burn)	2001 (after burn)
Unburned (1, 2, 3)	12.7 (\pm 6.0)	8.3 (\pm 1.8)	N/A	N/A	7.0 (\pm 3.1) ^a	8.3 (\pm 2.4) ^a
Burned(1B, 2B, 3B)	6.3 (\pm 2.2)	7.4 (\pm 0.4)	0.8 (\pm 0.3)	0.6 (\pm 0.5)	1.5 (\pm 0.4)	0.7 (\pm 0.6)

Note: Standard errors are in parentheses (\pm). N/A, not available.

^aVegetation cover change associated with drought.

on burned plots in the short term (first three years) was 84% (Table I). *Larrea* and *Ambrosia* have varied fire responses. Although neither species is well-adapted to fire, *Larrea* tends to recover more quickly than *Ambrosia* (McLaughlin and Bowers, 1982; Brown and Minnich, 1986). *Larrea* is known to re-establish former cover within five years of fire (O'Leary and Minnich, 1981). Recovery may take much longer; up to 76 years in certain conditions (Abella, 2010). In ideal growing conditions, *Larrea* reaches reproductive maturity at 8–13 years (USDA Forest Service, 2011). Miriti *et al.* (2001) found that *Ambrosia* may meet reproductive conditions in absence of adult competition within five years of new germination.

Materials and methods

Point cloud collection and alignment

We collected t-LiDAR scans from unburned and burned plots with similar vegetation and soil-landform characteristics in

Table II. Optech ILRIS 3D laser scanner specifications

Optech ILRIS 3D	
Dynamic scanning range	3 m to 1500 m
Data sampling rate (measure rate)	2500 points per second
Laser wavelength	1500 nm
Beam divergence	0.00974°
Beam diameter	22 mm at 100 m
Minimum spot step (X and Y axis)	0.00115°
Scanner field of view (ILRIS-3D)	40° × 40°
Raw positional accuracy	7 mm at 100 m
Averaged positional accuracy (minimum of four scans)	4 mm at 100 m

September 2009, 11 years after prescribed fires were conducted. We scanned six plots used in previous research activities with overlapping scans from four different angles (Haubrock *et al.*, 2009). This process was repeated for each sample plot using an Optech ILRIS 3D laser scanner mounted on a tripod (Optech, 2010). Optech scanner specifications are listed in Table II. We scanned from different perspectives at the phenological low (i.e. when annual vegetation was dormant) to maximize ground returns and reduce vegetation interference. Each scan was executed with 4–7 mm point spacing at distances 3 to 25 m from the target vegetation within each sample. We captured an average of 9.3 million (\pm 3.1 million) point position measurements (XYZ_{*i*}; where *i* is the intensity or infrared reflectivity of the target) for each of the six field plots, equaling an average scan density of 23 360 (\pm 7680) points/m² across all plots.

T-LiDAR scans of the same plot were aligned and combined through an algorithm that generates a best-fit surface through the individual points in each scan and then minimizes the differences among common surfaces (Stock *et al.*, 2011) (Figure 2). We used the Polyworks best-fit alignment module and assigned a local reference frame to each sample plot (Bates *et al.*, 2008; InnovMetric, 2010). Six reflective field markers were placed in each sample plot and were used as common reference points to aid in alignment among the four overlapping scans.

Point cloud errors and edits

We found the vast majority of overlapping point measurements had a 3-mm point density and a sub-millimeter misalignment with few exceptions. Misalignment measures the standard deviation in the data differences between scans for each sample plot. Exceptions occurred where vegetation point measurements or low density point measurements were

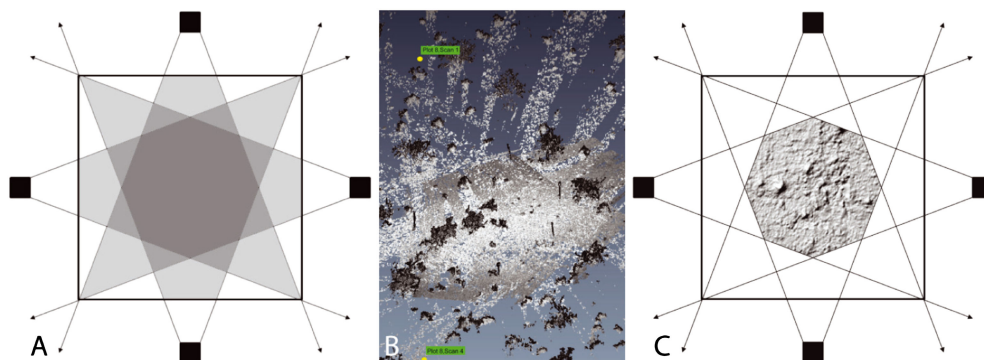


Figure 2. Overlapping point clouds created areas of higher point density with less shadows from surrounding vegetation. A conceptual birds-eye diagram (A) shows scanner locations as black boxes, scan path, and a grading color scale to illustrate where the most scan overlap occurs. Aligned scans that initially include all raw point cloud values for each plot (B) have higher point density towards the center of the plot. Once all of the vegetation and noise was removed (accounting for roughly 50% of the total points), a bare earth surface for the center of each plot (C) provided the basis for measuring mound volumes. This figure is available in colour online at wileyonlinelibrary.com/journal/espl

misaligned by 1 to 5 cm. We determined that wind likely shook the vegetation and produced enough angular changes in the vegetation to create the positional uncertainties we measured. Additionally, small angular misalignments from areas where data density was lower (< 1 cm spot spacing) produced noise in the dataset. Areas with excess wind noise and unacceptable data density were excluded from the mound and vegetation analysis. With over 56 million point measurements, it was crucial to remove additional pre- and post-alignment 'noise' to improve analysis and expedite data processing. Far-field data and data echoes were manually screened and removed prior to alignment. Post-alignment noise removal included the exclusion of low intensity data and remaining data echoes, which accounted for removal of approximately 10% of the original points. Although we feel confident that many of the error sources were identified and resolved, we acknowledge that additional errors associated with surface geometry or reflectivity may have an impact on the positional accuracy of the point data described here (Hodge *et al.*, 2009).

Mound and vegetation measurements

In previous studies of surface roughness using t-LiDAR, vegetation was physically removed prior to scanning to provide a direct line-of-sight between the t-LiDAR unit and the soil surface (Eitel *et al.*, 2011; Sankey *et al.*, 2011). In our case, vegetation was retained for immediate and long-term measurements. Digital vegetation filtering was also necessary for the geo-surficial component of our research (Sithole, 2001; Sithole and Vosselman, 2004). Terrascan software was used post-alignment to remove vegetation and alignment markers by experimenting with three filtering thresholds (Terrasolid, 2010). Filtering thresholds remove points at a specified distance (0 cm, 5 cm, and 10 cm) above the most dense ground surface points. Vegetation may be missed if the threshold is too high (10 cm), and ground points may be removed if the threshold is too low (0 cm). During the vegetation removal process, we found that the 5 cm filter created a bare-earth surface with few remaining vegetation points and without removing ground points. In total, the Terrascan filtering routine removed nearly 47% of the points from each plot's aligned point cloud.

Mound perimeters (or extents) were calculated by isolating the ground points that fell within the drip area for individual (or assemblages of) plants (Figure 3). We acknowledge that this underestimates plant mounds because plant-related topography often extends beyond vegetation canopy (Bedford and Small, 2008), and especially so in cases where plants have been reduced by fire. Generally, mound areas are roughly proportional to plant canopy area (Parsons *et al.*, 1992). Mound volumes were determined by measuring a triangulated irregular network (TIN) of the selected bare earth points (within the mound perimeter) relative to the plot-level plane. A plot-level plane was drawn for each plot by selecting the lowest points on the periphery of the plot. In most cases, a single plane was sufficient because the plots lacked topographic relief (except for the mounds). Abnormal volume measurements derived from this technique were resolved by creating a refined plane under each mound to account for localized relief changes.

Vegetation point cloud returns were retained for comparative analysis using a two-part process using Polyworks software (InnovMetric, 2010). We used the point cloud intensity values to isolate vegetation returns above the bare earth model. We then manually removed field markers and fence returns (peripheral to this project). This process resulted in a point cloud appropriate for plant height and radius measurements.

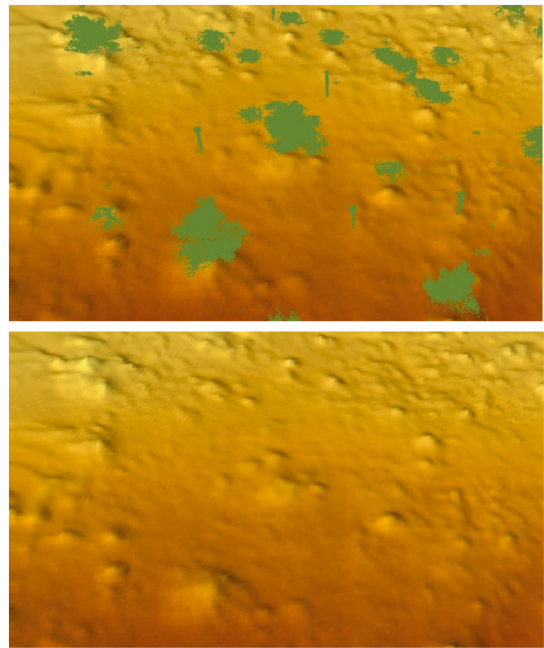


Figure 3. Example bare earth digital elevation model (DEM) without (lower panel) and with vegetation returns (upper panel) for burned plot (3B). Vegetation is shown in green. Surface is displayed as shaded relief with lighter colors representing higher elevations. This figure is available in colour online at wileyonlinelibrary.com/journal/espl

Plant height was measured by comparing each plant's point cloud to the plot plane from the base of the plant to the farthest point in the z-axis. Plant radius was measured by generating a line vector through the point cloud for each plant.

Surface roughness

In addition to mound and plant metrics, we calculated the soil-surface roughness for each plot (Bedford and Small, 2008). The measure of soil roughness is the elevation of the ground surface relative to a plane fit to the ground surface, thus providing a metric of ground surface variability. We quantified roughness (microtopography) with the variable Z_m , which is calculated with all LiDAR bare-earth returns, and normalized to have a mean of zero. We log-transformed Z_m to approximate a normal distribution by first adding a nominal value (100) to Z_m values to prevent the logarithm of a negative value. Because we defined Z_m as having the same mean value (zero for raw data, $\log_{10}(100)$ for transformed values), we tested for differences using F -test combinations between all pairs of plots. Tests were performed with transformed values, yet we only present results in untransformed values. Positive Z_m values are points above the plane fit to all the elevations of the plot, and negative values are below. The variability of Z_m can be thought of as roughness: areas with high roughness have high variability in Z_m and areas with low roughness have low variability (Figure 4). For this report, surface roughness is reported on the scale of centimeters, thus Z_m reflects differences in topography due to mounds, pits, rills, rocks, etc.

We also performed variogram analysis on microtopography (Z_m) data to quantify the magnitude and extent of spatial structure. We use Z_m values because the effects of surface slope of the plot areas have been removed with the Z_m method. This effectively removes a strong trend signal that would have been present if raw elevation values were analyzed. The techniques used here are described fully in Bedford and Small (2008). Due to the extremely large number of data points in the t-LiDAR point clouds, we used a random subset of 10 000 points from

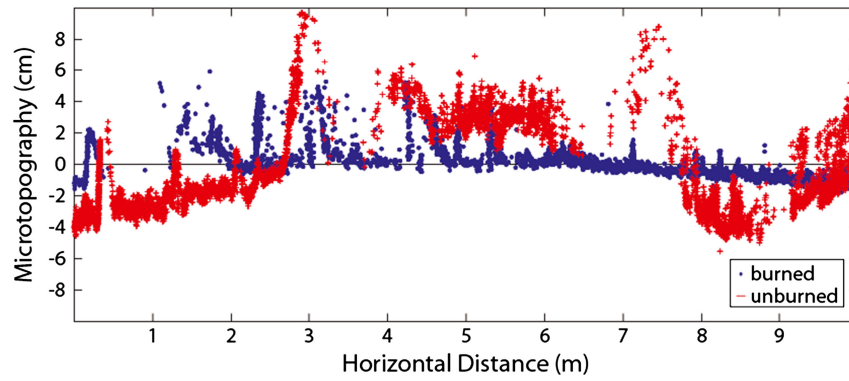


Figure 4. Cross-sections showing reduced height of plant mounds (large positive areas) and smoother roughness between mounds for a burned compared to unburned plot (5× vertical exaggeration). This figure is available in colour online at wileyonlinelibrary.com/journal/espl

each plot for variogram analysis. Experimental variograms were calculated in GSLIB (Deutsch and Journel, 1998) with a lag separation distance of 25 cm. Theoretical variograms were fit using weighted least squares of lag uncertainty with the R (version 2.1.4.0) statistical package with the fitting library NLME (Pinheiro and Bates, 2000). We use the range and sill parameters from the theoretical variograms of measures of the extent and magnitude of spatial structure of roughness, respectively.

Statistical analysis

We employed a heteroscedastic *t*-test (assuming unequal variances) to determine whether mound and vegetation metrics (mound volume, mound perimeter, vegetation height, and vegetation radius) differ between unburned and burned plots. We also conducted an *F*-test to determine if the variances for each of the four measurements were equal between the unburned and burned plots. Pearson correlations were measured between all measurements to detect a relationship between mounds and corresponding vegetation. Finally, we employed a series of linear regressions to further analyze the relationship between plants and mounds. Following the logic of published articles where the presence of plants leads to more wind deposition of potential mound material (Ravi *et al.*, 2009) and less water erosion (Eitel *et al.*, 2011), we hypothesize that the removal of vegetation will result in the opposite effect, reduced mound volume. Mound volume was treated as the dependent variable (*y*) against mound perimeter, plant height, and plant radius (*x*) in single and multiple linear regression tests. We derived regressions where the intercept was not set to zero, since we found cases where some small plants did not have mounds.

Results

T-LiDAR laser obstructions, misalignment between scans, and low intensity points led to the exclusion of roughly half of the mounds and corresponding plants (hereafter referred to as mound/plant pairs) we measured on plots from the analysis. The areas that were retained for measuring mound volumes and mound perimeters met our minimum point density requirement of < 1 cm spot spacing (10 000 points/m²). Once the obstructions, misalignments, and sources of potential noise in the LiDAR point clouds were identified and removed, we were able to gather measurements of mound volume, mound perimeter, plant height, and plant radius for 69 locations within the six plots (Table III). Across all 69 mound/plant pairs, the average number of XYZi points used for mound perimeter and

Table III. Mound volumes and perimeters, and corresponding plant heights and radii, were measured in 31 unburned mounds and 38 burned mounds within the unburned and burned plots

Plots	Volume (m ³)	Volume error (± m ³)	Perimeter (m)	Plant height (m)	Plant radius (m)	
<i>Unburned</i>						
Plot 1	0.191	0.021	11.43	1.30	1.55	
	0.009	< 0.001	2.71	0.50	0.30	
	0.061	0.007	5.56	0.60	1.03	
	0.028	0.003	2.57	0.40	0.41	
	0.032	0.004	3.04	0.40	0.47	
	0.188	0.021	8.76	1.30	1.53	
	0.076	0.008	5.27	0.80	—	
	0.035	0.004	2.83	0.55	0.44	
	0.173	0.019	9.17	1.25	—	
	0.105	0.012	6.19	1.10	—	
	0.027	0.003	2.90	0.40	—	
	Plot 2	0.036	0.003	3.04	0.50	0.45
		0.014	0.001	3.50	0.35	0.60
		0.068	0.006	5.34	0.90	0.75
0.018		0.002	2.50	0.40	0.35	
0.329		0.030	7.93	1.20	1.24	
0.042		0.004	3.66	0.30	0.55	
0.083		0.008	5.25	0.55	0.80	
0.028		0.003	3.44	0.40	0.38	
0.177		0.016	7.10	1.30	1.06	
0.046		0.004	3.27	0.40	0.49	
Plot 3	0.321	0.030	8.89	1.25	1.19	
	0.032	0.004	2.89	0.55	0.44	
	0.029	0.003	3.38	0.55	0.44	
	0.019	0.002	2.13	0.35	0.24	
	0.014	0.002	2.67	0.35	0.33	
	0.328	0.036	10.27	1.20	1.62	
	0.039	0.004	3.43	0.35	0.55	
	0.066	0.007	4.44	0.45	0.59	
	0.103	0.011	6.13	1.00	1.00	
	0.028	0.003	5.89	0.95	0.81	
<i>Burned</i>						
Plot 1B	0.008	0.001	2.37	0.35	0.37	
	0.135	0.020	10.38	1.10	1.82	
	0.064	0.009	4.71	0.45	0.67	
	0.015	0.002	3.11	0.45	0.40	
	0.019	0.003	3.03	0.50	0.44	
	0.003	< 0.001	1.47	0.30	0.24	
	0.072	0.011	4.28	0.60	0.62	
	0.040	0.006	3.32	0.40	0.56	
	0.006	0.001	2.57	0.35	0.37	
	0.285	0.042	9.75	1.15	1.42	
	0.011	0.002	1.76	0.40	0.30	

(Continues)

Table III. (Continued)

Plots	Volume (m ³)	Volume error (\pm m ³)	Perimeter (m)	Plant height (m)	Plant radius (m)
Plot 2B	0.031	0.005	3.33	0.45	0.53
	0.017	0.003	2.56	0.45	0.41
	0.019	0.003	2.39	0.45	0.39
	0.016	0.002	2.49	0.30	0.34
	0.021	0.003	2.55	0.35	0.39
	0.037	0.005	2.95	0.45	0.35
	0.031	0.004	3.09	0.50	0.42
	0.026	0.003	4.24	0.35	0.76
	0.013	0.002	2.82	0.45	0.36
	0.004	< 0.001	1.65	0.40	0.43
Plot 3B	0.026	0.003	3.58	0.50	0.54
	0.103	0.013	7.43	0.95	1.14
	0.147	0.019	9.51	1.00	1.64
	0.099	0.013	8.00	1.10	1.35
	0.020	0.003	3.98	0.65	0.62
	0.024	0.003	3.51	0.60	0.47
	0.014	0.001	3.25	0.45	0.47
	0.084	0.007	6.60	0.90	1.00
	0.019	0.002	3.20	0.45	0.48
	0.005	< 0.001	2.20	0.30	0.32
	0.008	< 0.001	2.42	0.30	0.34
	0.054	0.005	6.44	1.00	0.96
	0.009	< 0.001	2.51	0.35	0.37
	0.016	0.001	2.90	0.45	0.37
	0.038	0.003	3.50	0.55	0.68
0.034	0.003	2.98	0.45	0.40	
0.080	0.007	4.90	0.75	0.64	

Note: Perimeter, height, and radius measurements have an accuracy of ± 4 mm.

volume measurements was between 3000 and 150 000 points per mound. The average number of points for vegetation height and radius measurements was 9000 to over one million points per plant.

Mounds and plant measurements

In 31 unburned mound/plant pairs, the mean mound volume was $0.088 \text{ m}^3 (\pm 0.095)$, with a range of 0.009 m^3 to 0.329 m^3 . Shrubs growing on the mounds resulted from re-sprouts of previously established shrubs. We did not record any recruitment of newly established perennial shrubs on the burned mounds. The shrubs located on the unburned mounds had a mean height of $0.71 \text{ m} (\pm 0.36)$ and mean radius of $0.73 \text{ m} (\pm 0.41)$. In the 38 burned mound/plant pairs, the mean mound volume was less than half of the unburned mounds ($0.043 \pm 0.054 \text{ m}^3$, range of 0.003 m^3 to 0.285 m^3). The shrub vegetation was also reduced in burned plots, with mean height of $0.55 \text{ m} (\pm 0.25)$ and mean radius of $0.61 \text{ m} (\pm 0.39)$ (Figure 5). We determined that vegetation that had re-sprouted in previously burned plots was roughly 80% of the size of vegetation in unburned plots, while the mounds in burned plots were smaller by 50%.

Surface roughness

Although all plots had similar vegetation and soil-landform characteristics, we found differences in soil-surface roughness between some of the plots (Figure 6). Statistical tests (*F*-test) on log-transformed *Z*_m values (our roughness metric) show that unburned plots tend to have higher ranges of microtopography (more surface roughness), and that microtopography on unburned has higher variance as well. These data suggest that burned plots have decreased soil roughness compared to unburned plots, which have likely been smoothed via wind and water erosion following fire treatments.

We also used variograms to quantify the spatial structure of microtopography. Variograms and variogram parameters are presented in Figure 7. Variograms of *Z*_m from unburned plots were quite different than burned plots. In general, variograms from unburned plots have smaller ranges and larger sills, suggesting more spatial structure over somewhat smaller areas. Burned plots tended to exhibit smaller spatial structure (i.e. more homogenous) over large distances. The scale and

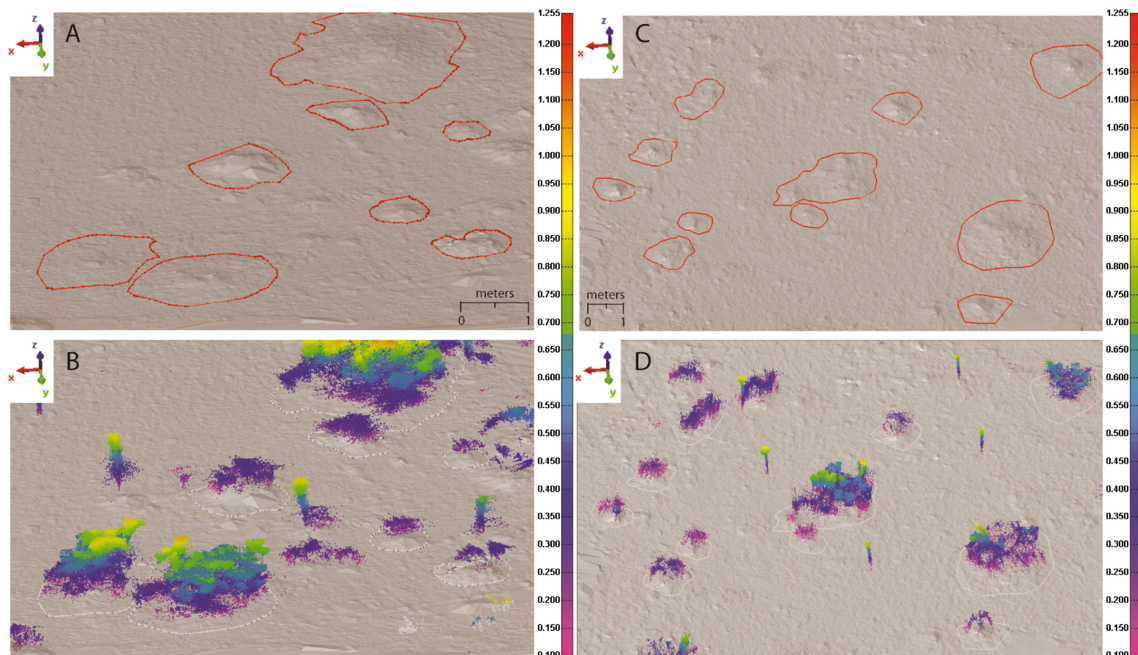


Figure 5. Bare-earth surface mound measurements for unburned plot 3 (A) and burned plot 3B (C) have corresponding vegetation height (B) and radius measurements (D). Heights ranged from 0.35 to 1.3 m for unburned vegetation (shrubs shown above have a maximum height of 1.1 m) and ranged from 0.3 to 1.15 m for burned vegetation (shrubs shown above have a maximum height of 0.95 m). This figure is available in colour online at wileyonlinelibrary.com/journal/espl

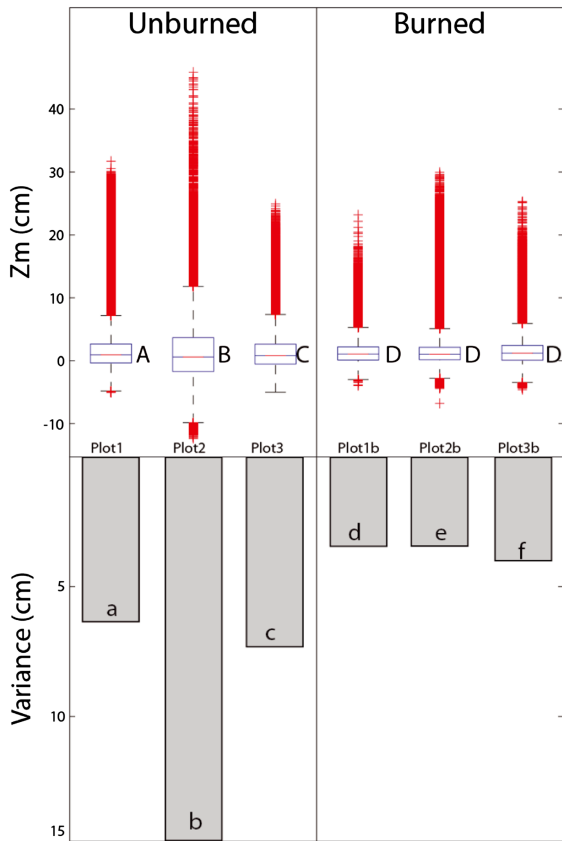


Figure 6. Surface roughness (Z_m) and its variance for each of the plots. For box plots, center lines are the median, box widths are the 25% quartiles, whiskers are data limits and red crosses are outliers. Capital letters denote significant differences in means, lowercase letters denote significant differences in variances, both at the 95% confidence interval. This figure is available in colour online at wileyonlinelibrary.com/journal/esp

magnitude of unburned microtopography is similar to other observations in creosotebush shrublands where vegetation plays a prominent role in forming small-scale soil properties including microtopography (Bedford, 2008; Bedford and Small, 2008).

The microtopography data suggest that fire alters the soil surface topography by reducing surface roughness lower and increasing homogeneity. Fire also alters the spatial structure of roughness. Burned plots have less structural magnitude and the smoother surfaces in these plots increase in extent. Effectively, fire and post-fire wind and water erosion likely cause the diffusion of the soil surface.

Relationship between mounds and plants

We found that mean mound volumes and plant heights are statistically distinct between unburned and burned plots ($T < 0.05$). Mean mound perimeters were only found to be different at $T < 0.10$, and the mean plant radii were not statistically different between unburned and burned plots ($T = 0.09$ and $T = 0.27$, respectively).

Correlations were high in each pair-wise comparison (Table IV). Based on the strong correlation between mound and plant dimensions, the hypothesis that plant size influences mound volume was tested in a series of linear regressions. Plant radius was found to be the best single determinant of mound volume across all samples ($R^2 = 0.731$). At the 99% confidence level ($P < 0.01$), every meter increase in radius results in a 0.209 m^3 increase in mound volume ($y = 0.209x - 0.064$). Plant height was also found to be a good determinant of mound volume across all samples ($R^2 = 0.701$). At the 99% confidence

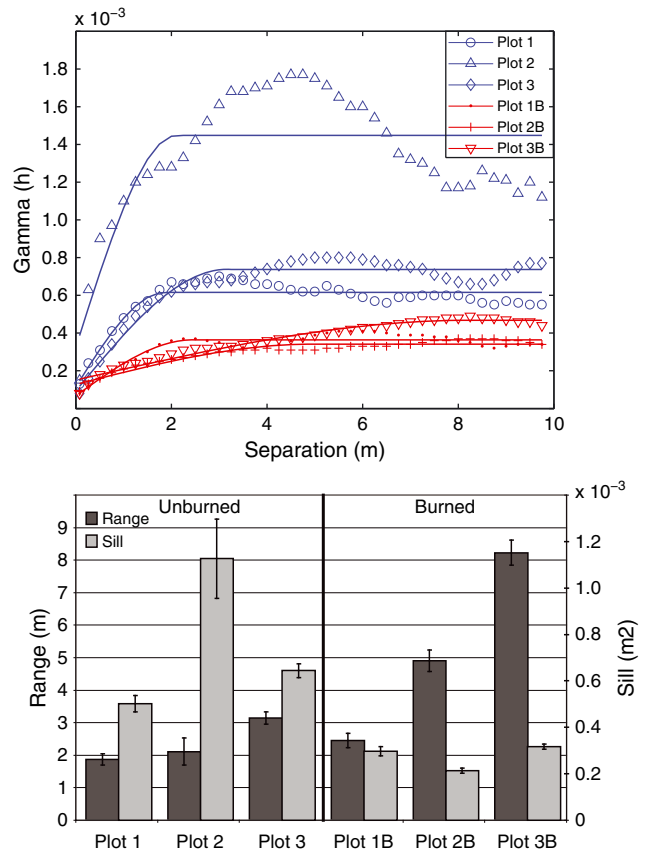


Figure 7. Variograms for unburned plots (blue) and previously burned plots (red), fit to theoretical models, suggest that roughness values are more spatially homogenous for burned plots across different scales. Burned plots also exhibit a lower semi-variance value (sill) and higher separation distance (range) relative to unburned plots. This figure is available in colour online at wileyonlinelibrary.com/journal/esp

Table IV. Correlation matrix for unburned and burned plots comparing mound measurements and plant measurements

	Volume	Perimeter	Radius	Height
<i>Unburned</i>				
Volume	1	—	—	—
Perimeter	0.87	1	—	—
Radius	0.86	0.98 ^a	1	—
Height	0.83	0.92	0.89	1
<i>Burned</i>				
Volume	1	—	—	—
Perimeter	0.89	1	—	—
Radius	0.84	0.98 ^a	1	—
Height	0.83	0.94	0.91	1

^aCollinearity was found between the mound perimeter and plant radius measurements due to similar use of plant canopy to derive measurements: mound perimeter was derived by using the plant drip area as the perimeter.

level ($P < 0.01$), every meter increase in height results in a 0.208 m^3 increase in mound volume ($y = 0.208x - 0.065$). Combining plant height and plant radius across all samples as combined variables in a multiple linear regression improves the coefficient of determination relative to the plant height alone (adjusted $R^2 = 0.716$). Combining plant height and plant radius across in a multiple regression for burned samples had an adjusted $R^2 = 0.715$. Combining plant height and plant radius across in a multiple regression for unburned samples had an adjusted $R^2 = 0.738$. Multiple linear regression results are shown in Table V.

Table V. Results of multiple linear regression with dependant variable (mound volume) and independent variables (plant height and radius)

Description	Intercept		Plant height		Plant radius	
	Coefficient	P-Value	Coefficient	P-Value	Coefficient	P-Value
All mounds	-0.066	< 0.001	0.139	0.001	0.067	0.027
Unburned mounds	-0.045	0.001	0.088	0.061	0.065	0.035
Burned mounds	-0.075	0.002	0.101	0.117	0.129	0.027

Note: The ANOVA *F*-test for variance difference between independent variables showed statistical significance for all three regressions ($F < 0.01$).

Discussion

In this study, t-LiDAR proved to be an effective way to remotely measure small soil mounds, plant dimensions, and surface roughness in a rapid data collection effort. Mound and corresponding vegetation measurements derived from LiDAR point data indicate that the presence of fire, or more specifically, the biogeomorphic processes that occur after fire, affect mound and plant disintegration/recovery in the Mojave Desert. Mound volumes and soil roughness were reduced on burned plots relative to unburned plots. We interpret these results to be caused by wind erosion, water erosion, or both, resulting from the lack of protection from vegetation canopy in burned plots. Our observations have certainly captured a change in shrub/mound size relationships due to erosional processes. A series of vegetation measurements indicate that recovery of shrub size is occurring slowly. However, because we made measurements on mound metrics during a single point in time we do not currently know if the mounds are stable, recovering, or continuing to disintegrate in relation to the plants. Considering observations of measured growth rates in the burned plots between 1998 and 2000 (Esque, 2004) and the field measurements taken during the 2009 t-LiDAR collection, we assume that plant cover was not fully recovered in burned plots 11 years after the prescribed fires were conducted. We conclude that although recovery is still occurring, *Larrea tridentata* and *Ambrosia dumosa* plant cover in the burned plots is reduced compared to unburned plots.

The loss of plant cover from fire has far reaching implications. Plant cover protects fertile mounds and preserves surface roughness (Eitel *et al.*, 2011), and the loss of plant cover exposes mounds and rough surfaces to erosion. Reduced vegetation canopy following fire promotes erosion which can essentially erase soil heterogeneity (in soil physical and nutrient characteristics) that shrubs promote as a positive feedback (Ravi *et al.*, 2009). This homogenization of the landscape likely has several effects. Smooth surfaces provide fewer safe-seed sites thus reducing seed residence times, inhibiting seed germination, plant establishment, and recruitment. Enhanced erosion also disturbs recovering vegetation and can reduce seed banks further. In addition to the reduced seed bank by heat exposure following fire (Esque *et al.*, 2010b), nutrient dynamics following fire favor establishment of invasive annuals (Esque *et al.*, 2010a). Vegetation canopies also provide micro-environments to protect biota from predators (Thomson, 1982) or thermal extremes (Lowe and Hinds, 1972), more favorable micro-environments as nurse plants (Drezner, 2007), and moisture retention (Walker *et al.*, 2001). Soil-surface roughness promotes retention of water that may be lost in runoff events through storage in microtopographic depressions (Bedford, 2008). Burned surfaces are less protected by vegetation and may be more susceptible to raindrop impacts as a result (Wainwright *et al.*, 1999; Sankey *et al.*, 2011). Although we did not simulate precipitation events, rainfall on exposed surfaces may contribute to the smoother surfaces that we measured in the burned plots. Loss of vegetation, mound, and surface roughness following fire may ultimately lead to feedback

mechanisms that can result in ecosystem degradation and shifts in ecosystem types (i.e. to annual grass-dominated systems).

Our results suggest that elimination of plant cover from fire, along with slow plant regrowth, has contributed to a reduction in mound volume and surface roughness. We did not explore the alternate scenario of mechanical vegetation removal; however, Sankey *et al.* (2011) addressed this question. Mechanical removal of vegetation resulted in more surface roughness (Sankey *et al.*, 2011), but these findings may only counter our measurements for burned areas because of differences in erosional and depositional patterns between study sites (Sankey *et al.*, 2010). Although we did not directly test how the elimination of plant cover from fire contributed to the reduction in mound volume and surface roughness, previous research suggests that the absence of vegetation affects surface morphology by exposing soils to wind and/or water erosion (Eitel *et al.*, 2011; Sankey *et al.*, 2011). Plant canopies protect the soil surface from erosion (Eitel *et al.*, 2011), and post-fire vegetation recovery promotes the re-establishment of soil heterogeneity (Bolling and Walker, 2000; Cammeraat *et al.*, 2010).

Without a complete record of past conditions in the study plots, we are unable to quantify the amount of soil loss following fire, or whether new vegetation growth occurred on pre-existing mound locations or not. Although our morphometric measurements illustrate a clear linkage between vegetation and soil surface topography, our brief study cannot determine the current trajectory of the mounds. But given the previously established relationships between vegetation and mounds, it seems that the stability or expected increase in plant size would result in mound recovery (growth). Alternatively, factors such as drought or other factors that decrease the size of the shrubs would send the process in the other direction.

The link between plant canopy size and mound size is not surprising given the processes that lead to mound formation (Bochet *et al.*, 2000). The primary processes are erosion of soils below plants, differential rain splash (Wainwright *et al.*, 1999; Furbish *et al.*, 2009), and wind deposition (Ravi *et al.*, 2007). In this arid system, rodents and the threatened desert tortoise are primary agents of bioturbation. The wholesale reduction in mound size due to physical factors may influence the presence or absence of these environmental engineers in ways that are currently unknown. Such ecosystem changes lead to much-discussed questions about biological and physical feedbacks in dryland patchy vegetation systems (Schlesinger *et al.*, 1990; Tongway and Ludwig, 1994; Puigdefabregas *et al.*, 1999; Wilcox *et al.*, 2003; Ludwig *et al.*, 2005; Puigdefabregas, 2005; Turnbull *et al.*, 2008).

The scale of ecosystem change is also an important factor when considering potential, large-magnitude disturbances in these arid shrubland systems. Wainwright *et al.* (2000) suggest that plot-scale disturbance analyses may not represent the real-world well, but we contend that the impact of vegetation loss from fire at the mound-to-plot scale can function as a rough approximation for regional scale disturbances. Whether regional-scale drought or fire serves as the driver of change,

larger disturbances that result in vegetation degradation will likely result in a comparable increase in the scale of surface erosion. The erosion that may ensue after a disturbance at this scale may change the geomorphology of the landscape by creating homogenous, smooth soil surfaces, as we found in this study. Smoothing may also occur only locally (Sankey *et al.*, 2011), with higher likelihood of roughness at the macro-scale, such as rough rills, gullies, and arroyos (Abrahams *et al.*, 1995). Either way, hydrologic and aeolian transport mechanisms operating on a denuded landscape may lead to water re-allocation and redistribution of nutrients and seeds, thus changing future vegetation distributions in the desert (Bochet *et al.*, 2000; Turnbull *et al.*, 2008). The potential for irregular distributions of water, nutrients, and seeds under this regional-scale disturbance scenario describes a landscape that lacks connectivity and is more susceptible to desertification (Okin *et al.*, 2009).

Summary

In an application where other remote sensing tools (for example, aerial photography or airborne LiDAR) would have an insufficient spatial resolution and lack the ability to capture individual mounds through vegetation obstructions, terrestrial (ground-based) LiDAR captured enough mound and vegetation point data to gather structure measurements, quantify the relationship between mounds and plants, and to calculate the statistical differences in mounds and plants between burned and unburned plots. The high-resolution vegetation, soil volume, and soil roughness measurements collected in this study improve the overall understanding of biogeomorphic processes following disturbances in a number of ways. Our observations not only demonstrate that burned plots have reduced vegetation heights, mound volume, and soil roughness relative to unburned plots, but also chronicle the recovery of vegetation. Vegetation measurements collected with t-LiDAR expand upon previous records showing *Larrea tridentata* and *Ambrosia dumosa* species response rates (Esque, 2004). The singular point in time for which we collected mound morphology did not provide an opportunity to measure change with time and determine the stability or recovery of mound structure and size, but did demonstrate that shrub size appears to influence mound size during a decade post-fire, and begs the question of how dynamic the structure and morphology of the mounds may be.

Desertification is defined as the degradation of land productivity (Okin *et al.*, 2009). Vegetation recovery appears to be slow and this has been confirmed through several studies (Billings, 1990; Lovich and Bainbridge, 1999; Webb *et al.*, 2009), yet future repeat scans will allow us to monitor the recovery of mounds, vegetation, and surface roughness even further and garner additional insights into post-fire recovery and whether the recovery rates are indicative of degraded land productivity or considered normal for the Mojave Desert.

With coupled hydrologic and sediment-transport models, or the growing body of literature on recovery implications, our data may provide additional knowledge into how water and wind erosion processes alter soil morphology and plant recovery. Using our observations in conjunction with prior research, we speculate that the erosion following the elimination of plant cover from fire has contributed to a substantial reduction in mound volume and smoother surfaces at the plot-scale. Furthermore, recovering vegetation in burned plots is likely slowing the restoration of mounds due to prolonged exposure to wind and/or water erosion. In the future, surface volume and roughness measurements can be coupled with dust emission data or precipitation data to quantify the role of wind

erosion (Sankey *et al.*, 2011) or water erosion (Eitel *et al.*, 2011) on unburned and burned surfaces.

Acknowledgments—This interdisciplinary study was primarily supported by the US Geological Survey (USGS) Invasive Species Program and the USGS Recoverability and Vulnerability of Desert Ecosystems (RVDE) project. LiDAR activities were supported by the USGS Geographic Analysis and Monitoring Program. The authors thank Joel Sankey, Ryan Gold, Gerald Bawden, Ken Nussear, Richard Inman, Katherine Huxter, and Alicia Torregrosa of the USGS for their support and suggestions. Any use of trade, product, or firm names in this publication is for descriptive purposes only and does not imply endorsement by the US government.

References

- Abella S. 2010. Review: Disturbance and Plant Succession in the Mojave and Sonoran Deserts of the American Southwest. *International Journal of Environmental Research and Public Health* **7**(4): 1248–1284.
- Abrahams AD, Parson AJ, Wainwright J. 1995. Effects of vegetation change on interill runoff and erosion, Walnut Gulch, southern Arizona. *Geomorphology* **13**: 37–48.
- Bates KA, Rarity FA, Manning PL, Hodgetts D, Vila B, Oms O, Galobart A, Gawthorpe RL. 2008. High-resolution Lidar and photogrammetric survey of the Fumanya dinosaur tracksites (Catalonia): implications for the conservation and interpretation of geological heritage sites. *Journal of the Geological Society* **165**: 115–127.
- Bedford DR. 2008. Effects of Vegetation-related Soil Heterogeneity on Runoff, Infiltration, and Redistribution in Semi-arid Shrubland and Grassland Landscapes. PhD Dissertation, University of Colorado, Boulder, CO; 178.
- Bedford DR, Small EE. 2008. Spatial patterns of ecohydrologic properties on a hillslope-alluvial fan transect, central New Mexico. *Catena* **73**(1): 34–48.
- Belnap J, Lange OL. 2003. *Biological Soil Crusts: Structure, Function, and Management*. *Ecological Studies* **150**, 2nd edn, Springer-Verlag: Berlin; 525.
- van den Berg L, Kellner K. 2005. Restoring degraded patches in a semi-arid rangeland of South Africa. *Journal of Arid Environments* **61**: 497–511.
- Billings WD. 1990. *Bromus tectorum*, a biotic cause of ecosystem impoverishment in the Great Basin. In *The Earth in Transition: Patterns and Processes of Biotic Impoverishment*, Woodwell GW (ed.). Cambridge University Press: Cambridge; 301–322.
- Bochet E, Poesen J, Rubio JL. 2000. Mound development as an interaction of individual plants with soil, water erosion and sedimentation processes on slopes. *Earth Surface Processes and Landforms* **25**(8): 847–867.
- Bolling JD, Walker LR. 2000. Plant and soil recovery along a series of abandoned desert roads. *Journal of Arid Environments* **46**(1): 1–24.
- Boxell J, Drohan PJ. 2009. Surface soil physical and hydrological characteristics in *Bromus tectorum* L. (Cheatgrass) versus *Artemisia tridentata* Nutt. (Big Sagebrush) habitat. *Geoderma* **149**: 305–311.
- Brown DE. 1982. Biotic communities of the American southwest – United States and Mexico. Special Issue. *Desert Plants* **4**: 1–342.
- Brown DE, Minnich RA. 1986. Fire and changes in creosote bush scrub of the western Sonoran Desert, California. *American Midland Naturalist* **116**(2): 411–422.
- Cammeraat ELH, Cerdà A, Imeson AC. 2010. Ecohydrological adaptation of soils following land abandonment in a semi-arid environment. *Ecohydrology* **3**(4): 421–430.
- Cox JR, Morton HL, LaBaume JT, Renard KG. 1983. Reviving Arizona's rangelands. *Journal of Soil and Water Conservation* **38**: 342–345.
- DeFalco LA, Esque TC, Nicklas MB, Kane JM. 2010. Supplementing seed banks to rehabilitate disturbed Mojave Desert shrublands: where do all the seeds go. *Restoration Ecology*. DOI: 10.1111/j.1526-100X.2010.00739.x
- Deutsch CV, Journel AG. 1998. *GSLIB: Geostatistical Software Library and User's Guide*, 2nd edn, Oxford University Press: Oxford; 369.
- Drezner TD. 2007. An analysis of winter temperature and dew point under the canopy of a common Sonoran Desert nurse and the implications for positive plant interactions. *Journal of Arid Environments* **69**(4): 554–568.

- Eitel JUH, Williams CJ, Vierling LA, Al-Hamdan OZ, Pierson FB. 2011. Suitability of terrestrial laser scanning for studying surface roughness effects on concentrated flow erosion processes in rangelands. *Catena*. 10.1016/j.catena.2011.07.009
- Esque TC. 2004. The Role of Fire, Rodents and Ants in Changing Plant Communities in the Mojave Desert, Dissertation, University of Nevada, Reno, NV; 168.
- Esque TC, Kaye JP, Eckert SE, DeFalco LA, Tracy CR. 2010a. Short-term soil inorganic N pulse after experimental fire alters invasive and native annual plant production in a Mojave Desert shrubland. *Oecologia* **164**(1): 253–263.
- Esque TC, Young JA, Tracy CR. 2010b. Short-term effects of experimental fires on a Mojave Desert seed bank. *Journal of Arid Environments* **74**(10): 1302–1308.
- Frankel KL, Dolan JF. 2007. Characterizing arid region alluvial fan surface roughness with airborne laser swath mapping digital topographic data. *Journal of Geophysical Research* **112**: F02025. DOI: 10.1029/2006JF000644
- Furbish DJ, Childs EM, Haff PK, Schmeckle MW. 2009. Rain splash of soil grains as a stochastic advection-dispersion process, with implications for desert plant–soil interactions and land-surface evolution. *Journal of Geophysical Research – Earth Surface* **114**: F00A03. DOI: 10.1029/2009JF001265
- Hastings JR, Turner RM. 1965. *The Changing Mile*. University of Arizona Press: Tucson, AZ; 317.
- Haubrock SN, Kuhnert M, Chabrillat S, Güntner A, Kaufmann H. 2009. Spatiotemporal variations of soil surface roughness from in-situ laser scanning. *Catena* **79**: 128–139.
- Hilty JH, Eldridge DJ, Rosentreter R, Wicklow-Howard MC. 2003. Burning and seeding influence soil surface morphology in an Artemisia shrubland in southern Idaho. *Arid Land Resource Management* **17**: 1–11.
- Hodge R, Brasington J, Richards K. 2009. In situ characterization of grain-scale fluvial morphology using terrestrial laser scanning. *Earth Surface Processes and Landforms* **34**: 954–968.
- InnovMetric. 2010. PolyWorks: 3-D scanner and 3-D digitizer software from InnovMetric Software Inc., Version 11. <http://www.innovmetric.com/manufacturing/home.aspx> [1 December 2010].
- Jackson TJ, Schmugge TJ, Wang JR. 1982. Passive microwave sensing of soil moisture under vegetation canopies. *Water Resources Research* **18**: 1137–1142.
- Li J, Washington-Allen RA, Okin GS. 2010. Characterizing Effects of Wind Erosion on Soil Microtopography in Semiarid Grassland using Terrestrial Laser Scanning. Abstract B33B-0403 presented at 2010 Fall Meeting, AGU, San Francisco, CA.
- Lovich JE, Bainbridge D. 1999. Anthropogenic degradation of the southern California desert ecosystem and prospects for natural recovery and restoration. *Environmental Management* **24**: 309–326.
- Lowe CH, Hinds DS. 1972. Effect of paloverde (*Cercidium*) trees on the radiation flux at ground level in the Sonoran Desert in winter. *Ecology* **52**: 916–922.
- Ludwig JA, Wilcox BP, Breshears DD, Tongway DJ, Imeson AC. 2005. Vegetation patches and runoff-erosion as interacting ecohydrological processes in semiarid landscapes. *Ecology* **86**(2): 288–297.
- McLaughlin SP, Bowers JE. 1982. Effects of wildfire on a Sonoran Desert plant community. *Ecology* **63**(1): 246–248.
- Miriti MN, Wright SJ, Howe HF. 2001. The effects of neighbors on the demography of a dominant desert shrub (*Ambrosia dumosa*). *Ecological Monographs* **71**(4): 491–509.
- National Oceanic and Atmospheric Administration (NOAA). 2003. *Climatological Data for Arizona*. NOAA, National Climatic Data Center: Asheville, NC.
- Nizeyimana E, Petersen GW. 1998. Remote sensing application to soil degradation assessments. In *Methods for Assessment of Soil Degradation*, Lal R, Blum WH, Valentine C, Stewart BA (eds). CRC Press: New York; 393–405.
- O’Leary JF, Minnich RA. 1981. Postfire recovery of creosote bush scrub vegetation in the western Colorado Desert. *Madrone* **28**(2): 61–66.
- Okin GS, Parsons AJ, Wainwright J, Herrick JE, Bestelmeyer BT, Peters DC, Fredrickson EL. 2009. Do changes in connectivity explain desertification? *Bioscience* **59**: 237–244.
- Optech. 2010. Optech, ILRIS-3D laser scanner. <http://www.optech.on.ca/> [1 December 2010].
- Parsons AJ, Abrahams AD, Simanton JR. 1992. Microtopography and soil-surface materials on semi-arid piedmont hillslopes, southern Arizona. *Journal of Arid Environments* **22**: 107–115.
- Perez-Gutierrez C, Alvarez-Mozos J, Martinez-Fernandez J, Sanchez N. 2007. Modeling of soil roughness using terrestrial laser scanner for soil moisture retrieval. In *Proceedings, IEEE International Geoscience and Remote Sensing Symposium (IGARSS)*, Barcelona; 1877–1880.
- Pierson FB, Carlson DH, Spaeth KE. 2002. Impacts of wildfire on soil hydrological properties of steep sagebrush-steppe rangeland. *International Journal of Wildland Fire* **11**(2): 145–151.
- Pinheiro JC, Bates DM. 2000. *Mixed-Effects Models in S and S-PLUS*. Springer-Verlag: Berlin; 538.
- Puigdefabregas J. 2005. The role of vegetation patterns in structuring runoff and sediment fluxes in drylands. *Earth Surface Processes and Landforms* **30**(2): 133–147.
- Puigdefabregas J, Sole A, Gutierrez L, del Barrio G, Boer M. 1999. Scales and processes of water and sediment redistribution in drylands; results from the Rambla Honda field site in southeast Spain. *Earth-Science Reviews* **48**(1–2): 39–70.
- Rahman MM, Moran MS, Thoma DP, Bryant R, Holified Collins CD, Jackson T, Orr BJ, Tischler M. 2008. Mapping surface roughness and soil moisture using multi-angle radar imagery without ancillary data. *Remote Sensing of Environment* **112**: 391–402.
- Ravi S, D’Odorico P, Okin GS. 2007. Hydrologic and aeolian controls on vegetation patterns in arid landscapes. *Geophysical Research Letters* **34**(25): 5.
- Ravi S, D’Odorico P, Wang LX, White CS, Okin GS, Macko SA, Collins SL. 2009. Post-fire resource redistribution in desert grasslands: a possible negative feedback on land degradation. *Ecosystems* **12**(3): 434–444.
- Reynolds JF, Virginia RA, Kemp PR, de Souza AG, Tremmel DC. 1999. Impact of drought on desert shrubs: effects of seasonality and degree of resource island development. *Ecological Monographs* **69**(1): 69–106.
- Ritchie JC. 1995. Airborne laser altimeter measurements of landscape topography. *Remote Sensing of Environment* **53**: 91–96.
- Sankey TT, Bond P. 2011. LiDAR-based classification of sagebrush community types. *Rangeland Ecology & Management* **64**: 92–98.
- Sankey JB, Eitel JU, Glenn NF, Germino MJ, Vierling LA. 2011. Quantifying burning effects, roughness, and dust with laser altimetry at sub-meter scales. *Geomorphology* **135**: 181–190.
- Sankey JB, Glenn NF, Germino MJ, Gironella AN, Thakray GD. 2010. Relationships of aeolian erosion and deposition with Lidar derived landscape surface roughness following wildfire. *Geomorphology* **119**: 135–145.
- Schlesinger WH, Pilmanis AM. 1998. Plant–soil interactions in deserts. *Biogeochemistry* **42**(1–2): 169–187.
- Schlesinger WH, Reynolds JF, Cunningham GL, Huenneke LF, Jarrell WM, Virginia RA, Whitford WG. 1990. Biological feedbacks in global desertification. *Science* **247**(4946): 1043–1048.
- Sithole G. 2001. Filtering of laser altimetry data using a slope adaptive filter. *International Archives of Photogrammetry and Remote Sensing* **34-3/W4**: 203–210.
- Sithole G, Vosselman G. 2004. Experimental comparison of filter algorithms for bare-Earth extraction from airborne laser scanning point clouds. *ISPRS Journal of Photogrammetry and Remote Sensing* **59**: 85–101.
- Spaulding WG. 1990. Vegetational and climatic development of the Mojave Desert; the last glacial maximum to the present. In *Packrat Middens; the Last 40,000 years of Biotic Change*, Betancourt JL, Van Devender TR, Martin PS (eds). University of Arizona Press: Tucson, AZ; 166–199.
- Stock GM, Bawden GW, Green JK, Hanson E, Downing G, Collins BD, Bond S, Leslar M. 2011. High-resolution three-dimensional imaging and analysis of rock falls in Yosemite Valley, California. *Geosphere* **7**(2): 573–581.
- Terrasolid. 2010. TerraScan. <http://www.terrasolid.fi/en/products/terrascan> [1 December 2010].
- Thomson SD. 1982. Structure and species composition of desert heteromyid rodent species assemblages: effects of a simple habitat manipulation. *Ecology* **63**(5): 1313–1321.
- Titus JH, Nowak RS, Smith SD. 2002. Soil resource heterogeneity in the Mojave Desert. *Journal of Arid Environments* **52**: 269–292.
- Tongway DJ, Ludwig JA. 1994. Small-scale resource heterogeneity in semi-arid landscapes. *Pacific Conservation Biology* **1**: 201–208.
- Turnbull L, Wainwright J, Brazier RE. 2008. A conceptual framework for understanding semi-arid land degradation: ecohydrological interactions across multiple-space and time scales. *Ecohydrology* **1**(1): 23–34.

- USDA. 2007. Arizona – National Agriculture Imagery Program. http://www.fsa.usda.gov/Internet/FSA_File/az_naip_07cm.pdf [29 July 2011].
- USDA Forest Service. 2011. International Institute of Tropical Forestry, *Larrea tridentata*. <http://www.fs.fed.us/global/iitf/pdf/shrubs/Larrea%20tridentata.pdf> [1 June 2011].
- Wainwright J, Parsons AJ, Abrahams AD. 1999. Rainfall energy under creosotebush. *Journal of Arid Environments* **43**: 111–120.
- Wainwright J, Parsons AJ, Abrahams AD. 2000. Plot-scale studies of vegetation, overland flow and erosion interactions from Arizona and New Mexico. *Hydrological Processes* **14**: 2921–2943.
- Walker LR, Thompson DB, Landau FH. 2001. Experimental manipulations of fertile islands and nurse plant effects in the Mojave Desert, USA. *Western North American Naturalist* **61**: 25–35.
- Webb RH, Belnap J, Thomas KA. 2009. Natural recovery from severe disturbance in the Mojave Desert. In *The Mojave Desert: Ecosystem Processes and Sustainability*, Webb RH, Fensler LF, Heaton JS, Hughson DL, McDonald EV, Miller DM (eds). University of Nevada Press: Reno, NV; 343–377.
- Wilcox BP, Breshears DD, Allen CD. 2003. Ecohydrology of a resource-conserving semiarid woodland: effects of scale and disturbance. *Ecological Monographs* **73**(2): 223–239.